



Current research on thermochemical conversion of biomass at the National Renewable Energy Laboratory

Robert M. Baldwin^{a,*}, Kimberly A. Magrini-Bair^a, Mark R. Nimlos^a, Perrine Pepiot^a, Bryon S. Donohoe^b, Jesse E. Hensley^a, Steven D. Phillips^a

^a National Bioenergy Center, National Renewable Energy Laboratory, Golden, CO, USA

^b Biosciences Center, National Renewable Energy Laboratory, Golden, CO, USA

ARTICLE INFO

Article history:

Received 9 February 2011

Received in revised form 7 September 2011

Accepted 17 October 2011

Available online 25 October 2011

Keywords:

Biomass

Thermochemical conversion

Gasification

ABSTRACT

The thermochemical research platform at the National Bioenergy Center, National Renewable Energy Laboratory (NREL) is primarily focused on conversion of biomass to transportation fuels using non-biological techniques. Research is conducted in three general areas relating to fuels synthesis via thermochemical conversion by gasification:

- (1) Biomass gasification fundamentals; chemistry and mechanisms of tar formation
- (2) Catalytic tar reforming and syngas cleaning
- (3) Syngas conversion to mixed alcohols

In addition, the platform supports activities in both technoeconomic analysis (TEA) and life cycle assessment (LCA) of thermochemical conversion processes. Results from the TEA and LCA are used to inform and guide laboratory research for alternative biomass-to-fuels strategies. Detailed process models are developed using the best available material and energy balance information and unit operations models created at NREL and elsewhere. These models are used to identify cost drivers which then form the basis for research programs aimed at reducing costs and improving process efficiency while maintaining sustainability and an overall net reduction in greenhouse gases.

© 2011 Elsevier B.V. All rights reserved.

1. Introduction

One of the major thermochemical conversion routes for manufacture of transportation fuels from biomass that is being researched at National Renewable Energy Laboratory (NREL) consists of biomass gasification to create raw syngas followed by catalytic gas cleaning/conditioning to produce clean syngas suitable for downstream catalytic fuel synthesis [1–6]. Fig. 1 is a schematic of this process. The syngas cleanup step accounts for a significant portion of the cost of the production of fuels [7]; accordingly research is being conducted to increase the reliability and performance of the catalysts used in this step. Efforts are also underway to improve gasification to reduce the amount of tars in the raw syngas in order to reduce the demands on the cleanup step. Fuel synthesis, currently focused on ethanol, is then conducted with cleaned syngas and proprietary fuel synthesis catalysts. The

following sections discuss research being conducted at NREL in gasification, syngas cleanup and synthesis of mixed alcohols.

1.1. Gasification research

Biomass gasification research is focused on applications of low-temperature atmospheric pressure fluid bed and entrained-flow reactor technologies using both steam and recycle gas as the fluidizing/transport medium. The work is carried out over a broad scale ranging from laboratory microreactors through bench scale systems up to NREL's 20 kg/h thermochemical process development unit (TCPDU); a schematic of the TCPDU is shown in Fig. 2.

The TCPDU is very flexible, and can be used for studies of both gasification and pyrolysis in either the fluidized bed or entrained-flow mode of operation. To complement pilot studies conducted in the TCPDU, research on gasification fundamentals is conducted in the following general areas: chemical kinetics and mechanisms of gasification, heat and mass transport in reactors, and the chemical and physical changes occurring in biomass during gasification and the impact upon product evolution.

* Corresponding author.

E-mail address: Robert.Baldwin@nrel.gov (R.M. Baldwin).

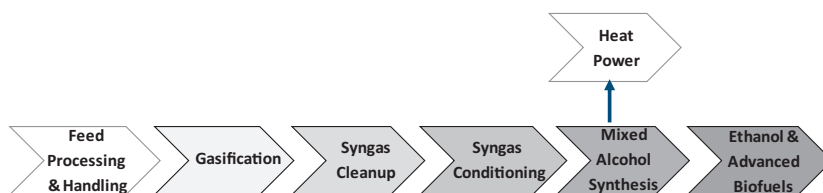


Fig. 1. A schematic of the conversion of biomass to biofuels through gasification and fuel synthesis.

1.2. Tar reforming catalyst development and syngas cleaning

Research on syngas cleaning has focused on the development of a novel nickel alumina based fluidizable tar reforming catalyst promoted with magnesium and potassium. This catalyst has been shown to be very effective in destroying tars and benzene via reforming (>99%) while also reforming methane (>90%) in a high-sulfur environment with all species reforming to produce more syngas. Performance of this catalyst has been verified at laboratory through pilot scales. This syngas cleaning approach eliminates the need for a downstream methane reformer while improving biomass carbon use. A companion strategy is the development of high-temperature sulfur sorbents at NREL as a way to reduce or eliminate deactivation of the reforming catalyst from exposure to hydrogen sulfide, which is generated during biomass gasification. A novel manganese-based sorbent that reduces H_2S from 1000 to 1 ppmv in simulated syngas at 700°C has been developed and has been tested successfully on biomass-derived syngas in the TCPDU. These NREL developed sorbents work in the high moisture environment associated with indirect steam gasification at operating temperatures to 700°C . Downstream reforming is viable at 700°C though better performance is achieved by reheating the syngas to reforming temperatures $\geq 800^\circ\text{C}$. While fluidized bed tar reforming without H_2S removal is efficient at temperatures $\geq 800^\circ\text{C}$, sorbent use more than doubles actual reforming time before regeneration is required. Technoeconomic analysis using pilot scale generated data is underway to determine which approach is more cost effective.

1.3. Syngas conversion to mixed alcohols

Fuel synthesis research is currently focused on improving metal sulfide catalysts, which can convert syngas to ethanol in a single reactor. Catalysts are being developed that are more selective for ethanol synthesis and more productive per loaded volume. Reaction products are being analyzed in detail for distillation properties and chemical composition so that the complexities of the crude alcohol product and fuel properties of the finished product can be understood. Catalysts are being tested in 'clean' and TCPDU-derived syngas to determine the sensitivity of the catalyst to poisons and to validate the level of syngas cleanup necessary for commercial operation. Mechanisms of mixed alcohol synthesis and associated kinetics are being developed to further improve our predictive process models, and catalyst lifetime and deactivation studies are being conducted to improve the current understanding of protection and regeneration protocols. Additional research is being conducted with several industrial partners, with emphasis on validating the performance of development stage and commercial ready mixed alcohol catalysts. All activities interface with NREL's technoeconomic analysis (TEA's) team, and provide data that improves and/or validates performance and cost projections. Future work will investigate synthesis of fuels with an emphasis on high-density infrastructure-compatible materials – specifically hydrocarbons in the naphtha, diesel, and jet boiling ranges.

In the following narrative, NREL's thermochemical conversion research comprising improvements in indirect gasification to

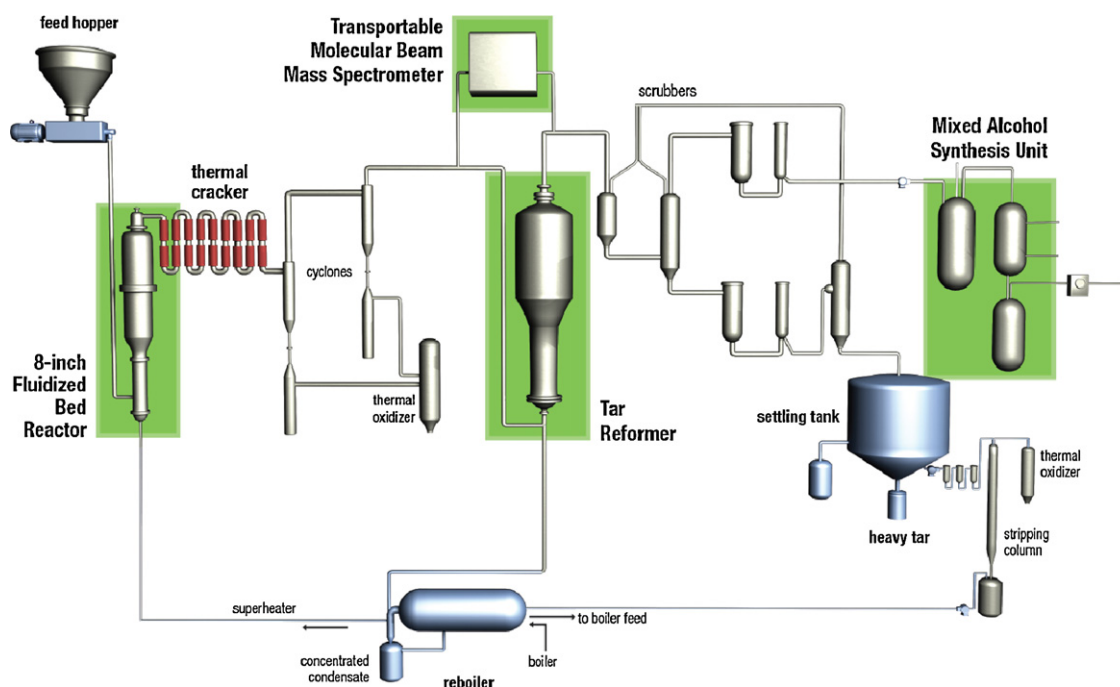


Fig. 2. NREL's thermochemical process development unit (TCPDU).

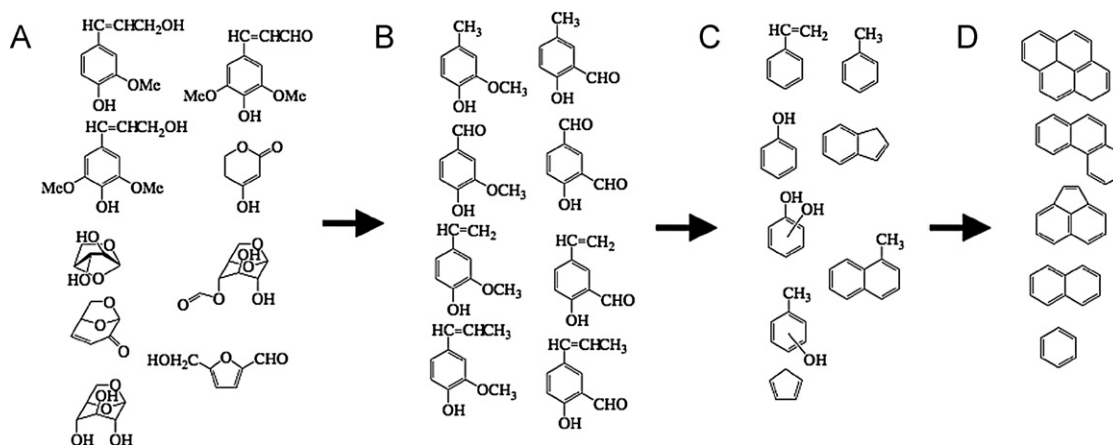


Fig. 3. Representative molecular species showing evolution of tars during pyrolysis. (A) At low temperatures (500–600 °C) primary pyrolysis products are formed. (B and C) These products crack at intermediate temperatures (600–700 °C) to smaller molecules. (D) PAHs are formed at higher temperatures (700–900 °C).

reduce tar formation, tar reforming catalyst development, syngas cleaning, and catalytic ethanol synthesis is outlined in more detail.

2. Formation of biomass-derived gasification tars

Tars, defined as condensable organic molecules (C_6 and greater), are pervasive in syngas from biomass gasification because the process is usually conducted at moderate temperatures (700–900 °C) where complete cracking of the tars is not possible. These tar compounds deactivate fuels synthesis catalysts, clog transfer lines and damage compressors creating the need for a cleanup step after gasification to remove tars as well as methane and other hydrocarbon contaminants. However, this is often expensive due to the high cost of effective catalysts. Modifying the gasification step to produce less tar can help reduce the demands on the reforming catalysts, improving performance and cost of this step.

The tars formed at typical gasification temperatures are primarily polycyclic aromatic hydrocarbons (PAHs – benzene, naphthalene, phenanthrene, anthracene, etc.) as well as some methylated aromatics [8–11]. These compounds are problematic for two reasons; (1) they are very stable, refractory, and difficult to crack further and (2) they can be precursors for coke formation on catalyst surfaces. As a result, NREL has focused on understanding the chemistry of tar formation with the objective of finding ways to reduce the formation of PAHs during the gasification step. This approach additionally reduces the catalyst tar reforming load. As discussed below, the unique mechanisms for the formation of these molecules provides an opportunity to adjust gasifier conditions so as to reduce their concentrations.

2.1. Characterization of tars

The tars formed during biomass pyrolysis include a wide range of molecular species; formation of these compounds during gasification has a strong dependency on the gasifier temperature. Evans and Milne [11] measured the products from the pyrolysis of biomass in hot helium using a Molecular Beam Mass Spectrometer (MBMS), and showed clear trends in the types of species that were formed as a function of the temperature of the helium. As the temperature was increased from 500 °C to 900 °C, the primary pyrolysis products first cracked, and eventually formed PAHs at high temperatures. These observations have been confirmed with MBMS measurements from a laminar entrained flow reactor (LEFR)[8] and pilot scale fluidized bed reactor [9,10]. In all of these studies, multivariate analysis was used to identify correlated groups of intermediates in this transformation to PAHs. Fig. 3 shows trends

in the evolution of representative products as a function of temperature. At the lower temperatures primary pyrolysis products of the individual components of biomass (lignin, cellulose and hemicellulose) are observed. These molecules have a significant amount of oxygen and many have high molecular weights. As the temperature is increased, these products are cracked, the molecular weight decreases and the amount of oxygen in the products decreases. These cracking reactions also result in the formation of the useful syngas components (CO and H_2). Eventually, small hydrocarbon molecules and radicals recombine to form PAHs through mechanisms that have been demonstrated in hydrocarbon combustion chemistry; these PAHs are prevalent in the tars that are observed during biomass gasification. It is reasonable to expect that similar trends in tar formation will occur as a function of residence time at gasification temperatures (700–900 °C). At the earliest times the primary pyrolysis products evolve from the biomass, these products are cracked and then as time progresses small hydrocarbons and radicals recombine to form PAHs.

The mechanisms of tar formation and destruction are of critical importance in determining the concentrations of PAHs in the syngas. Tar cracking reactions are dominated by unimolecular decomposition mechanisms. Model compound studies [12,13] have shown that these bond breaking, rearrangement and elimination reactions often involve the loss of CO and hydrogen. At higher temperatures, many of these reactions result in the formation of small hydrocarbons or radicals. Often the radicals are resonance stabilized such as propargyl radical ($C_3H_3^{\bullet}$) and cyclopentadienyl radical ($C_5H_5^{\bullet}$). Since they are stable, they build up at high temperatures and react with other molecules to form PAHs. Thus, the formation of PAHs is dominated by bimolecular and termolecular reactions. Because of the prevailing mechanism, the rate constants for the cracking reactions are independent of concentration, while the reactions that lead to the formation of PAHs are strongly dependent upon the concentration of the tars. As a result, in the regions within a gasifier where tars and tar cracking products build up there is a greater potential for PAH formation. If tars can be quickly dispersed into the product stream within the gasifier reactions can be directed away from PAH formation.

2.2. Biomass structure and PAH formation

The structure of plant material potentially plays an important role in the rates of release of products from biomass and the formation of PAHs due to transport limitations. At a practical level, this was recently demonstrated at NREL with experiments that measure the products from gasification with spherical particles of wood of

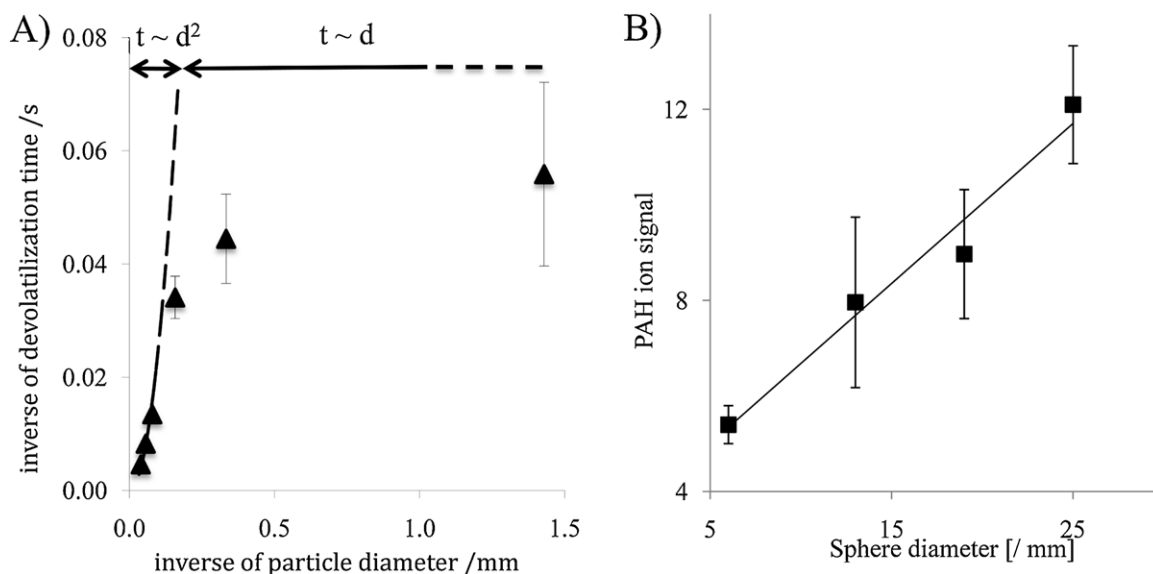


Fig. 4. Results from the gasification of oak spheres at 800 °C. (A) Evolution of carbon monoxide as a function of sphere diameter. (B) The formation of total PAHs from spheres with different diameters as measured with an MBMS. Experimental standard deviations are shown in (B).

varying sizes [14]. Fig. 4a shows a plot of the devolatilization time, that is, the time needed for all volatiles to escape from the heated wood particle as a function of the particle diameter. Given the range of sizes investigated, two modes could be observed. For large diameters, the devolatilization time scales with the particle diameter squared, indicating internal heat and mass transfer limitations. This behavior transitions toward a linear variation with diameter for smaller particles, as external heat and mass transfer become the limiting factors [15]. These experiments also showed for a given amount of wood a decreased yield of syngas with increased sphere size, and a slight increase in the formation of PAHs at gasification temperatures (Fig. 4b). These observations are consistent with other literature results [15–17].

The results of these studies suggest that minimizing mass and heat transport effects by reducing the biomass particle size is desirable for improving gasification efficiency and reducing tar production. Typically, woody feedstocks are delivered to biomass processing facilities as chips with dimensions on the order of several centimeters. Further reduction in size requires mechanical energy and increases the overall cost of the process. Thus, the process cost savings of using smaller particles needs to be weighed against the size reduction costs. In any event, this dependence of yield upon particle size is a clear indication of heat and mass transfer restrictions placed upon the gasification process. An understanding of transport restrictions imposed by the architecture of plant cell walls can help lead to process improvements.

Mass transport is restricted by the tissue and cellular structure in plant matter. Vascular bundles that transport water, minerals and organic material throughout plants provide a greater conductance along the grain, while transverse conductance is more difficult. The cells that make up the vascular tissue are elongated with the dimensions of the inner lumen of the cell in the range of 10–100 μm in the dimensions transverse to the growth axis and 100 s of μm along the growth axis of the plant. The sclerenchyma cells that provide mechanical support have similar dimensions, but are not as elongated. Cell senescence of these tissues leads to a loss of organelles and other protein material inside the cell resulting in an empty cell lumen. Thus, in dead plant cells the dense cell walls or the pits (1–10 μm) in these walls generally limit mass transport in biomass.

It is hypothesized that this cellular mass transport restriction coupled with the tar chemistry discussed above can lead to

enhanced tar formation during biomass gasification. It has been demonstrated with microscopy that during gasification and pyrolysis the overall plant tissue architecture remains intact. At pyrolysis temperatures (<600 °C) the cell walls tend to thin as material is volatilized. In order to be useful these volatilized products must escape from the cell lumen through pits or ruptures in the cell walls created during pyrolysis [16]. Microscopic imaging has shown that if the vapors do not escape, they can condense into tar microspheres inside the charred cells. Fig. 5 shows a light microscopic image of a pyrolyzed plant cell with trapped microspheres and Fig. 6 shows a schematic of this process. These tar microspheres can eventually react further to form char and thus contribute to lower carbon efficiency for the process. Under gasification conditions, the high concentration of pyrolysis products entrapped in the cell lumen can also lead to the formation of PAHs, since formation of these species

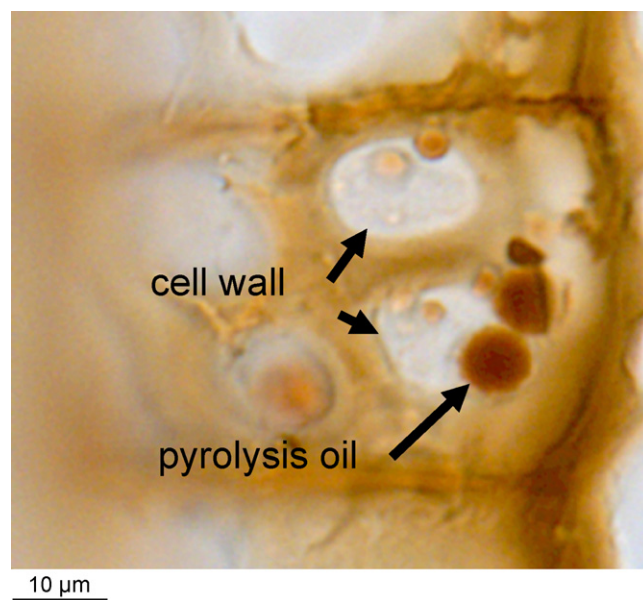


Fig. 5. TEM image showing the formation of tar microspheres after the pyrolysis of poplar.

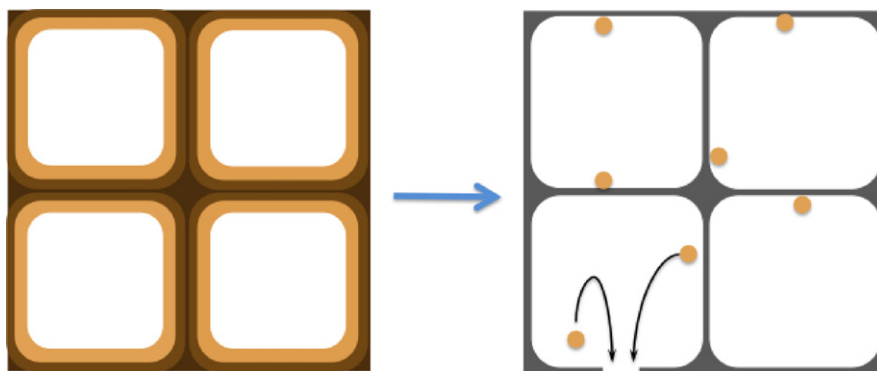


Fig. 6. A model showing the pyrolysis of plant cells. The plant walls thin as material is volatilized. The vapors can be trapped in the lumen of the plant cells.

is favored by high concentrations. Thus, build up of pyrolysis vapors in the lumen of cells during gasification could lead to increased PAH formation relative to the situation in which these vapors successfully escaped the biomass particle into the reactor. This observation potentially provides an explanation for why larger particles tend to produce more PAHs.

Mass transfer restrictions occurring in the plant cell walls themselves may also contribute to enhanced PAH formation during gasification. A simple calculation based upon bulk density of biomass ($\sim 0.5 \text{ g cm}^{-3}$) and the void volume of the lumen ($\sim 80\%$) shows that the density of material in the plant cell walls is approximately 2 g cm^{-3} . Thus, diffusion of materials through or out of these walls will be difficult. When rapidly heated it is well known that biomass becomes plastic and as a result, gases evolved in the plant cell wall during gasification can form bubbles [8]. These bubbles contain pyrolysis vapors and may also provide an opportunity for the buildup of the concentration of species that lead to the formation of PAHs. Practical biomass particle size reduction would be ineffective for reducing this type of mass transport because plant cell walls are too small, $1\text{--}10 \mu\text{m}$, and grinding particles to sizes smaller than this dimension would be prohibitively expensive.

2.3. Fluid dynamics in a fluidized bed and PAH formation

While intra-particle phenomena impact the nature of the compounds released from the biomass particles, the ultimate fate of these species is dictated by the flow dynamics inside the gasification reactor. As mentioned before, PAH formation is a relatively slow process and mostly proceeds through temperature-sensitive, endothermic bimolecular reactions [17]. It is therefore favored by longer residence times inside the hot reactor environment [8], and locally high concentrations of precursors such as small hydrocarbon species and single-ring aromatics. As a result, several important factors at the reactor scale will affect the ultimate tar yield in the raw syngas, including gas phase residence time distribution and mixing characteristics for both the solid and the gas phases. Those factors are directly linked to the large-scale hydrodynamic structures inside the reactor. Fluidization of a bed of solid particles such as olivine sand results in pockets of low particle volume fraction, or bubbles, which expand and grow as they rise through the bed. While these bubbles greatly contribute to solid mixing by recirculating the particles, they also introduce some local inhomogeneities that can affect the amount of tar formed. For example, recent experimental and numerical studies of fluidization have shown that the bubbling pattern strongly depends on the fluidization intensity, with fewer and smaller bubbles observed at low inlet gas velocities [18–20]. This behavior is illustrated in Fig. 7 using computational fluid dynamics. More details on the Lagrange–Euler approach used in the simulations can be found in [20].

Interestingly, it was found using CFD that the bubbling intensity directly correlates with the width of the gas residence time distribution (RTD) function [20]. Fig. 8 shows that for inlet gas velocities close to the minimum fluidization velocity, the RTD, centered on the bulk residence time, remains quite narrow, thereby mimicking a plug flow reactor. However, as the velocity is increased, gas entrapped in a bubble will be carried quickly through the bed with little contact with the surrounding solids, while primary biomass devolatilization products evolved from the biomass particles may remain trapped inside denser, hot parts of the bed up to nearly four times the bulk residence time, providing ample time for the primary products to decompose and recombine to form PAHs.

This suggests that due to the bubbling process inherent to gas–solid fluidization, a non-homogeneous gas mixture will exit the bed, which may impact PAH levels. Solids segregation also poses a challenge. The differences in size and density between the biomass particles, up to a few inches long and relatively light, and the fluidizing sand, much heavier with a diameter of the order of a few hundred microns, are notable. Even if the biomass is injected at the bottom of the reactor, it may rise and float on top of the bed, thereby reducing significantly the heat transfer to the particles, widening the range of conditions experienced by the gasifying

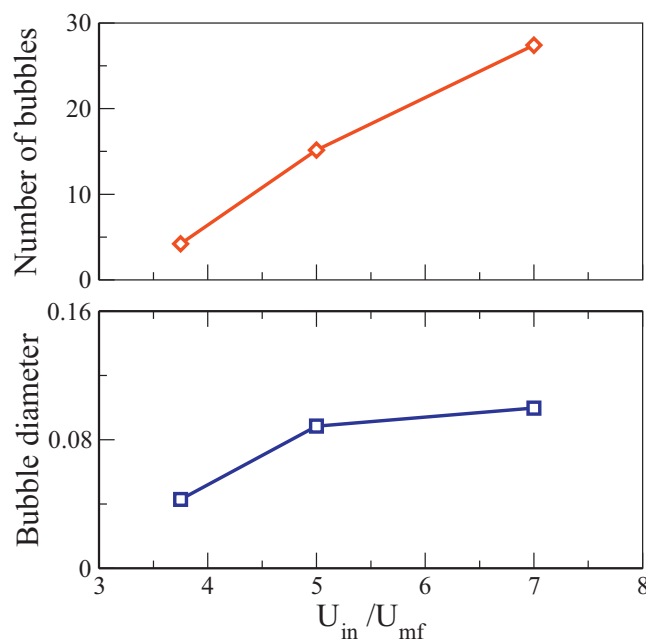


Fig. 7. Evolution of bubble number and size as function of inlet gas velocity obtained from numerical simulations. Fluidizing gas is injected with a uniform inlet velocity (porous plate) [20].

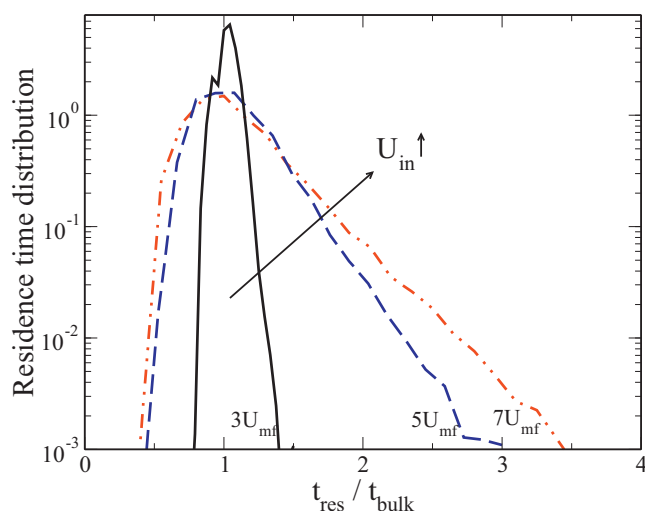


Fig. 8. Residence time distribution for different inlet gas velocities obtained from numerical simulations. Black = 3 times minimum fluidization velocity (U_{mf}), blue = $5 \times U_{mf}$, red = $7 \times U_{mf}$.

biomass, and lowering the products residence time inside the reactor. Additional work is under way to quantify the contribution of the flow dynamics to product composition using numerical tools.

3. Tar reforming catalyst development

Catalytic reforming of the hydrocarbon contaminants in raw syngas to additional carbon monoxide and hydrogen results in higher carbon utilization of the biomass feedstock and a higher carbon efficiency. This requires that the catalyst be able to reform recalcitrant tars, olefins and methane, which can make up to 20 vol% (dry basis) of syngas generated by low temperature steam gasification of biomass. Catalytic conditioning of biomass-derived syngas by steam reforming has been studied on catalysts developed at NREL [21–24] and elsewhere [27–29]. Supported nickel-based catalysts with various promoters have been the most widely studied class of materials and generally show good initial activity, but are susceptible to deactivation from contaminants in raw syngas such as hydrogen sulfide, ammonia, hydrogen chloride, tars, and other trace contaminants. These impurities require removal, usually through catalytic conditioning, in order to produce a quality syngas for end-use synthesis of liquid fuels such as ethanol and hydrocarbon fuels. The syngas conditioning component of the overall biomass to fuels process being developed at NREL is based on a fluidizable reforming catalyst that can handle conditions that will be experienced in recirculating reactors without appreciable attrition. This NREL-developed material has been evaluated for reforming performance with both biomass derived and model syngas and in fixed bed and recirculating reactor configurations with the goal of identifying the best catalyst composition and reactor type for a pilot scale process demonstration in 2012. General results from testing of this catalyst are discussed below.

4. Experimental

4.1. Tar reforming catalyst preparation

The attrition resistant catalyst used in this work is the most active composition developed to date at NREL for reforming tars and methane in raw biomass-derived syngas. A mechanically stable support material consisting of alpha alumina particles of 90% purity and 100–250 μm particle size was used to prepare a 75 kg

Table 1

Oak-derived and model syngas reactant compositions used in pilot and laboratory scale catalyst testing.

Species	Actual syngas (vol%)	Model syngas (vol%)
H ₂	27.13	30.00
CH ₄	14.60	15.00
CO	33.65	30.00
CO ₂	18.36	18.50
C ₂ H ₂	0.49	
C ₂ H ₄	4.62	6.42
C ₃ H ₆	0.12	
C ₃ H ₈	0.95	
1-C ₄ H ₄	0.07	
Benzene	0.002357	0.075
Total	100.00	100.00

batch of Ni-based catalyst. Catalyst composition, modeled on commercial naphtha reforming catalysts, contained 2.4 wt% Mg, 6.0 wt% Ni and 3.9 wt% K. An aqueous mixture of nickel (Ni), potassium (K) and magnesium (Mg) nitrate salts (99% Ni (NO_3)₂·6H₂O, Mg (NO_3)₂·6H₂O (Alfa Aesar), and 99% KNO₃ (Aldrich) was added to the support particles via incipient wetness. The wet solids were dried and calcined at 650 °C in air in a rotary continuous feed calciner to decompose the metal salts into the corresponding metal oxides. MgO and K₂O remain as oxides on the surface. Nickel oxides are reduced to catalytic metal species on the support surface in hydrogen at 850 °C prior to reforming. An earlier variant of this catalyst comprising 6.1 wt% Ni, 3.9 wt% MgO, and 4.6 wt% K₂O was used to assess reforming performance of ethylene as a tar surrogate in a fixed-bed microactivity test system (MATS).

4.2. Bench-scale tar reforming and regeneration

The MATS reactor was designed and constructed at NREL to rapidly test catalyst reforming activity. This system was used to assess tar reforming activity and catalyst self regeneration via a series of experiments that explored the effect of hydrogen sulfide concentration first on ethylene only as a tar surrogate then on methane conversion in model syngas. The MATS system [22] is an automated reactor capable of conducting multiple sequential reactions with a fixed catalyst bed (0.1–2 g). Varied syngas compositions, simulating the pilot scale biomass derived syngas (see Table 1), are mixed via a mass flow controlled manifold and delivered to the reactor. Steam was delivered from water supplied to an ultrasonic nozzle located above the catalyst bed. All process data were recorded by an OPTO 22 data acquisition system. Dried product gas was sampled every 4 min by an on-line Varian micro gas chromatograph that quantified helium (used as tracer gas), hydrogen, oxygen, nitrogen, methane, carbon monoxide, carbon dioxide, ethylene, ethane, benzene and acetylene. Product gas flow rates were calculated based on helium flow rate to the system and its concentration in the product gas. Carbon balances were calculated based on the flow rates and concentration of the gas components. In all MATS catalyst tests carbon closed within 99–101%.

4.3. Reforming and regeneration using biomass-derived syngas

Testing of reforming catalysts with raw biomass-derived syngas was carried out using a reaction system designated as SMARTS (Slipstream Micro Activity Reactor Test Stand). SMARTS was designed to operate on either a slipstream of syngas from the TCPDU or from bottled gases to evaluate small quantities (1–10 g) of reforming catalysts, sulfur sorbents, and regeneration protocols at temperatures up to 1200 °C. Gas temperatures were measured by thermocouples inserted into the reactor through fittings at the inlet and outlet and positioned to be near the bed on the inlet side

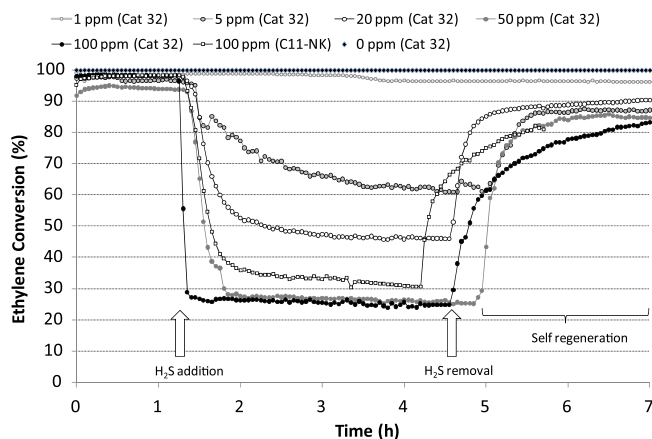


Fig. 9. MATS reforming catalyst performance testing with model syngas (Table 1), 0.5 g of Ni-based catalyst (6.1 wt% Ni, 3.9 wt% MgO, 4.6 wt% K₂O), pure ethylene, 0.8 g/min of steam, GHSV of 90,000 h⁻¹, and H₂S added at 1, 5, 20, 50, and 100 ppmv. Steady state ethylene conversion without H₂S was >99% using these reforming conditions.

and in the empty tube on the outlet side. The catalyst was supported on a double layer of fine mesh stainless steel screen in each reactor with a thin layer of quartz wool on top of the catalyst bed; reactors were operated in down flow mode. Analysis of permanent and light hydrocarbon gases was performed using a combination of gas chromatography, infrared spectroscopy (for CO, CO₂, CH₄), and thermal conductivity (for H₂).

Syngas from the TCPDU typically contains entrained char particles and high molecular-weight tar with a dew point around 450 °C. All process lines must be heated to above the dew point to prevent blockages from the gradual accumulation of tar and char particles. Heated vessels containing sintered-metal filters (nominal pore size of 2 μm) were used to remove most of the entrained char TCPDU slipstream.

The syngas was generated in the TCPDU using oak pellets as the biomass feedstock. The TCPDU was operated in the “entrained flow” mode where biomass was fed directly into the thermal cracker, bypassing the fluidized bed; a typical syngas composition is shown in Table 1. For some tests methane was added to the slipstream to increase its concentration in the gas to about 6 vol% to match more closely the concentration at the reformer inlet when recycle gases are sent to the reformer. Twenty sccm of argon was added as a tracer to the syngas between the TCPDU take off point and the SMARTS to accommodate estimating the total volumetric gas flow.

5. Results and discussion

5.1. Effect of H₂S on ethylene reforming

Ethylene is a refractory tar surrogate and was used to assess the impact of hydrogen sulfide levels on both catalyst reforming activity and the extent of activity recovery by regeneration. Fig. 9 shows MATS performance testing of 0.5 g of catalyst with an earlier version of reforming catalyst (6.1 wt% Ni, 4.6 wt% K₂O, 3.9 wt% MgO on Al₂O₃) at 850 °C, with pure ethylene, 0.8 g/min of steam, GHSV of 90,000 h⁻¹, and H₂S added at 1, 5, 20, 50, and 100 ppmv. Süd Chemie's C11NK reforming catalyst was evaluated for comparison.

Initial ethylene conversion was greater than 95% with conversions dropping rapidly as H₂S was added to the ethylene feed; steady-state reforming in H₂S was found to be a function of H₂S concentration. When only H₂S was removed from the feed gas, each catalyst self-regenerated to provide ethylene conversions of 80% or greater though regeneration time varied depending on H₂S concentration.

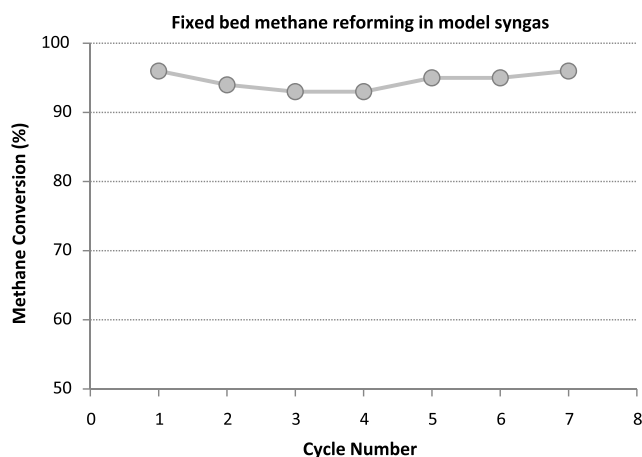
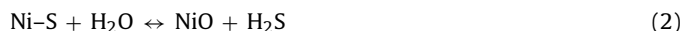


Fig. 10. Reforming performance with methane in model syngas in the MATS system.

Sulfur is known to selectively adsorb and form metal sulfides on many materials. The deactivation of Ni catalysts through sulfur poisoning has been studied by many groups [25–27] and has been attributed to the formation of nickel sulfides (Ni_xS_y). Both this work on nickel/alumina (Ni/Al₂O₃)-type catalysts exposed to H₂S and that of other authors indicate that a nickel sulfide (or, in general, a metal sulfide) can be regenerated with steam to form H₂S and a metal oxide [28–31] followed by reduction in H₂ to recover the reduced metal as shown in Eqs. (1)–(3).



This preliminary work with ethylene reforming has been reproduced with model syngas containing methane, which is more recalcitrant to crack than ethylene, as the tracking species for reforming efficiency. These results also demonstrate both the impact of H₂S on reforming rate and the ability of this catalyst to self regenerate in a process stream containing steam and model syngas components. Subsequent work has focused on regenerating deactivated catalysts with varied syngas components (steam, CO, CH₄, CO₂, H₂) to guide pilot-scale reforming and regeneration experiments in the TCPDU with raw syngas.

5.2. Methane and tar reforming with regeneration; model syngas

As shown in Table 1, methane is present in significant quantity in syngas derived by indirect steam gasification of biomass. Accordingly, to maintain good carbon efficiency it is imperative that methane reforming activity of the tar reforming catalyst be as high as possible. In addition, it is expected that contaminants in biomass-derived syngas will deactivate the reforming catalyst necessitating periodic regeneration. To test for these factors methane reforming with a packed bed catalyst coupled with regeneration in model syngas was studied in the MATS system. Fig. 10 shows these results and plots the initial methane conversions obtained during each of the consecutive reforming/regeneration cycles. For these experiments a reaction cycle comprised reforming at 900 °C, 119,000 h⁻¹, and steam-to-carbon ratio of 7.5. Reforming was conducted for 40 min with 53 ppmv of H₂S added 10 min into the reforming cycle. Regeneration was conducted for 60 min at 850 °C with the same steam content and a GHSV of 114,000 h⁻¹. Reduction conditions were 850 °C for 30 min in 28% H₂ in inert. As can be seen, excellent methane reforming activity was maintained and the catalyst recovered essentially to its initial activity level after each regeneration

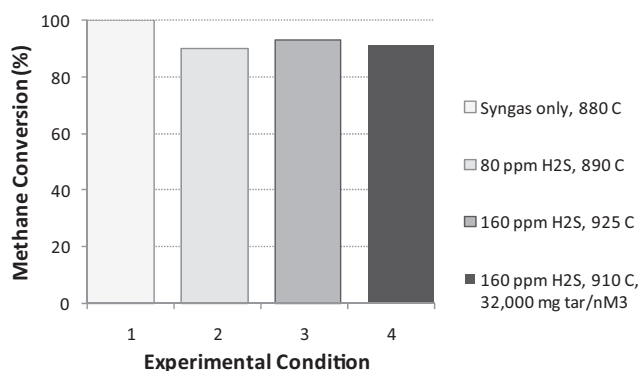


Fig. 11. Comparison of reforming/reaction cycles model syngas spiked with H₂S and tars in a recirculating regenerating system.

cycle was completed. Further work has shown that the regeneration and reduction steps can be combined using a combination of steam and hydrogen at 850 °C. This approach is currently being explored by evaluating the use of tail gas from the mixed alcohol synthesis step for regeneration.

Commercial-scale regeneration of catalysts within a fluidized bed reactor (such as those for fluid catalytic cracking processes) can be achieved using a recirculating/regenerating design in which the catalyst is continuously regenerated through use of separate reaction and regeneration zones. The rationale for this approach is that regeneration is both faster and more complete for short exposure times to reactant gases, in which sulfur interaction with the active nickel catalyst could be limited to surface reactions as opposed to bulk phase formations that could occur during longer periods of exposure. This hypothesis is also supported by recent work with 75 kg of a similar Ni-K-Mg/Al₂O₃ catalyst (manufactured by NREL) using recirculating/regenerating conditions in an industrial, pilot scale system in which steady-state tar and methane reforming activity were maintained (>90% conversion) in the presence of up to 160 ppmv H₂S. This system was operated under dry reforming conditions (approximately 3% steam) and at short catalyst/syngas contact times (minutes). Fig. 11 shows reforming results obtained with model syngas at 880 °C, syngas with 80 ppmv H₂S and 890 °C, syngas with 160 ppmv H₂S and 925 °C, and syngas containing surrogate tar species at a loading of 32,000 mg/nM³, reforming temperature of 925 °C, and 160 ppmv H₂S. These conditions were chosen to quickly assess the impact of multiple process changes (H₂S and tar content, reforming temperature) on methane conversion.

Steady state methane conversion for all test conditions was >90% at process temperatures ranging from 880 to 925 °C, H₂S content of 80–160 ppm, and a model tar content of 32,000 mg/nM³. Increasing the reforming temperature from 880 to 910 °C maintained >90% methane conversion in the presence of tar and H₂S. These results demonstrate that recirculating/regenerating reforming operations are able to effectively maintain high, steady-state catalyst activity for tar and methane reforming in the presence of H₂S at levels representative of actual biomass-derived syngas and support the process model of combined tar and methane reforming in one step.

5.3. Reforming and regeneration using biomass-derived syngas

The NREL tar reforming catalyst has also been tested in the SMARTS reaction system using syngas derived by indirect gasification of oak in steam at 850 °C. Reaction conditions evaluated included: (1) reforming at 900 °C with periodic regeneration and; (2) reforming at 950 °C with no regeneration. The reaction/regeneration protocol consisted of five cycles of reforming for

10 min followed by staged regeneration in steam and hydrogen according to the following procedure:

- 4 min: 8.7 vol% H₂, 65 vol% H₂O balance N₂
- 4 min: 65 vol% H₂O balance N₂
- 2 min: 50 vol% H₂ balance N₂

Fresh catalyst showed nearly complete (~100%) conversion of methane when first brought on line. After reforming for 10 min, the catalyst was regenerated for 10 min and then a second reforming period started immediately. The five reaction/regeneration cycles comprised a total operating time of approximately 100 min at 900 °C. A slow decline in recovered activity after each regeneration cycle was noted, but at the end of the 5th regeneration cycle the initial activity for methane conversion was still approximately 96%, indicating that very good reforming activity was being maintained by periodic regeneration. These results should be considered preliminary as much longer runtimes are required to determine the activity of the equilibrium catalyst.

A final set of experiments were conducted at 950 °C. Again, fresh catalyst activity was nearly 100% conversion for methane. The initial activity decreased rapidly when first exposed to syngas from the TCPDU, but at the higher temperature used in these runs, the catalyst activity reached a steady level and thereafter decreased very slowly; methane conversion was still greater than 91% after 7 h of continuous operation with no regeneration. These results suggest that the rate of catalyst poisoning by the biomass-derived syngas can be partially alleviated by operation at higher temperatures. Additional work is now in progress to optimize the need for regeneration vs. longer run times at higher temperatures.

6. Catalytic mixed alcohol synthesis

Mixed alcohol synthesis from syngas has been studied for several decades, and many catalysts that are capable of this chemistry have been discovered. Details of these catalysts can be found in recent reviews by Spivey and Egbebi and Subramani and Gangwal [32,33]. Biomass to ethanol process designs were considered by NREL several years ago, and an economic analysis suggested that the performance of mixed alcohol catalysts must be improved to ensure ethanol production at competitive prices [7,34]. After exhaustive literature reviews and discussions with process modelers, NREL chose to study and improve metal sulfide type catalysts. This choice was made for several reasons:

1. These catalysts already show competitive performance and require less improvement overall,
2. The metal sulfides are especially tolerant of syngas impurities and actually benefit from H₂S, which is ubiquitous in biomass derived syngas,
3. The cost of these materials, while high, is much lower than other alternatives like supported rhodium,
4. Alkali promoted sulfides have inherently low selectivities to methane, and
5. These materials have the potential for near term commercialization, including scaled synthesis and operation in proven reactor systems.

To understand and to improve the metal sulfide catalysts, NREL designed a number of bench and pilot scale differential and integral reactors for performance testing. These units allow testing at pressures up to 140 bar and temperatures up to 500 °C with custom blends of syngas or reformed gas from the TCPDU. In the 18 months since commissioning, the systems have provided nearly 10,000 h of catalyst testing, including long catalyst runs (>1000 h continuous

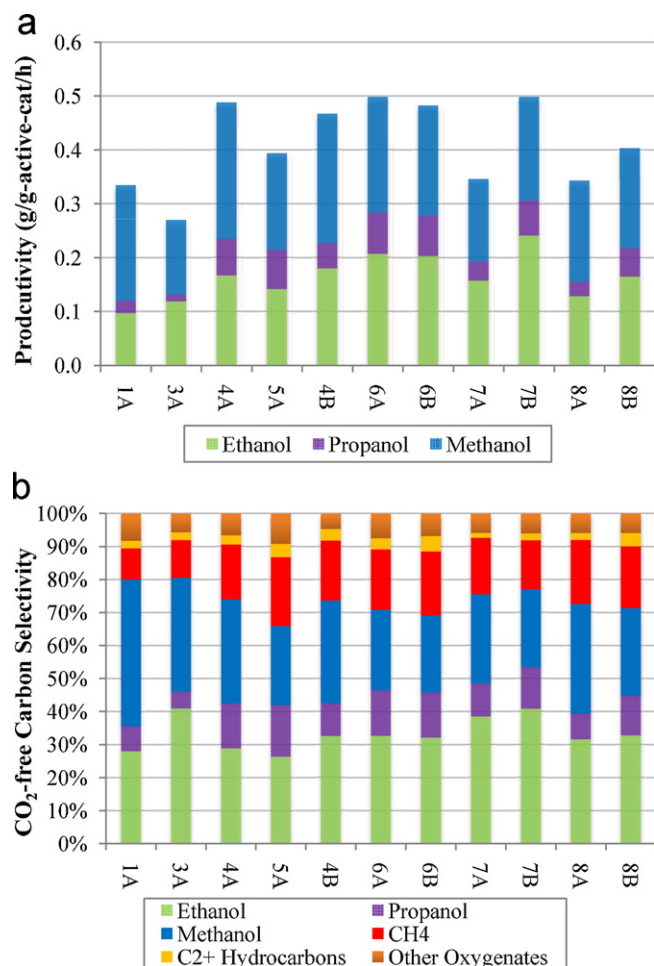


Fig. 12. Performance of NREL-formulated potassium-cobalt-molybdenum sulfide catalysts at 325 °C, 6000 NTPL/kg-cat/h gas flow, $p_{\text{CO}} = p_{\text{H}_2} = 700$ psi. All catalysts contain identical ratios/loadings of Mo, Co, and S. Catalysts 'A' and 'B' contain potassium in ratios of 1:1 and 0.7:1 K:Mo, respectively. Data shown for (a) alcohol productivity and (b) CO₂-free carbon selectivity (fraction of carbon incorporated in a product to carbon incorporated in all products).

operation), collection of kinetic data, and screening of several in-house and industrial catalyst formulations. Additionally, NREL has used its biomass catalyst characterization lab to determine fundamental relationships between catalyst preparation strategies and the performances of the finished materials. Fig. 12 shows performance results from several catalysts with identical metal sulfide compositions, but prepared in different ways using insights from the aforementioned fundamental research. The details of these fundamental tests and catalyst preparations are currently proprietary, but will be released in a number of publications to be submitted to the literature in coming months. Fig. 12 suggests that a metal sulfide catalyst can have widely variable performance depending on the methods used to prepare it. Some preparation techniques lead to improved activity, some lead to improved selectivity, and still others lead to improvements in both areas. All but two of the catalysts (catalysts 1 and 3) in Fig. 12 represent an improvement in performance to the best industrial catalyst known to NREL. Details of the economics of a biomass to ethanol plant using this industrial catalyst are provided in an extensive report recently released by NREL [35]. Assuming scalability of NREL's catalyst formulations, these improvements suggest that a sufficiently active and selective mixed alcohol catalyst is on the horizon.

A general theme of mixed alcohol catalysis research at NREL is that all work is done with commercialization in mind. Exotic

or challenging synthesis techniques, reactor geometries, process conditions, catalyst metals, or activation/regeneration procedures are not used. All efforts are made to envision use of catalysts at very large scale, including considerations of production, loading, operation, and decommissioning. NREL is also mindful of the market-readiness of the finished fuels the catalysts might make, and strives to develop catalysts that produce 'drop-in' products where possible. As examples, the following studies are underway, some near completion, all of which will appear in the literature soon:

- Reaction product liquids are being tested for major and minor components including sulfur species that result from catalyst deactivation. Minor components are being evaluated as suitable or unsuitable for fuel use to determine the levels of product finishing that might be required in a commercial facility. The nature and fate of sulfur through distillation is being evaluated as well, to determine if additional sulfur removal is necessary to produce a saleable fuel.
- Catalyst preparation strategies are being developed that decrease the number and/or complexity of synthesis steps. The aim of these studies is to decrease or eliminate the need for special equipment for producing these catalysts (i.e. not already in use by catalyst manufacturers), to improve quality and repeatability of catalyst syntheses, and to reduce the overall cost of synthesis.
- Data is collected within industrially-relevant operating ranges, such as moderate space velocities, temperatures, and pressures. This has the added benefit of providing more robust TEA analysis, as 'unproven' process equipment need not be modeled.

In coming years NREL will shift focus to production of hydrocarbon fuels from syngas, such as improved methods for synthesizing gasoline, diesel, or jet from syngas or syngas intermediates like methanol. As presently, NREL will keep a research strategy that is rooted in fundamentals but designed to push near-term commercialization of developed technologies.

7. Conclusions

NREL's program for thermochemical conversion of biomass is multi-faceted and encompasses diverse routes to transportation fuels and intermediates. Production of ethanol from cellulosic biomass via gasification and catalytic fuels synthesis has received significant development over the past several years, with syngas cleaning being an important research area in this project. To that end, NREL researchers have developed a novel tar and light hydrocarbon reforming catalyst that is robust and can be used in a recirculating/regenerating reactor configuration. This catalyst has demonstrated excellent tar and methane conversion efficiency on both model and biomass-derived syngas streams. Fundamental research into tar mitigation or elimination during biomass gasification is promising and may be used to reduce tar loads on the reformer catalyst. Research in catalytic conversion of syngas to mixed alcohols is ongoing, with steady improvements in catalyst performance and an ever-increasing understanding of catalyst function. The integrated process described here to thermochemically convert biomass to transportation fuels is scheduled for pilot scale demonstration at NREL in 2012.

References

- [1] L. Devi, K.J. Ptasinski, F. Janssen, Biomass Bioenergy 24 (2003) 125–140.
- [2] D.C. Dayton, A review of the literature of catalytic biomass tar destruction., National Renewable Energy Laboratory (NREL) Technical Report, Golden, CO, 2002.
- [3] Z. Abu El-Rub, E.A. Bramer, G. Brem, Ind. Eng. Chem. Res. 43 (2004) 6911–6919.

- [4] M.M. Yung, W.S. Jablonski, K.A. Magrini-Bair, *Energy Fuels* 23 (2009) 1874–1887.
- [5] D. Sutton, B. Kelleher, J.R.H. Ross, *Fuel Process. Technol.* 73 (2001) 155–173.
- [6] J.N. Kuhn, Z.K. Zhao, L.G. Felix, R.B. Slimane, C.W. Choi, U.S. Ozkan, *Appl. Catal. B-Environ.* 81 (2008) 14–26.
- [7] S.D. Phillips, *Ind. Eng. Chem. Res.* 46 (2007) 8887–8897.
- [8] M.W. Jarvis, T.J. Haas, B.S. Donohoe, J.W. Daily, K.R. Gaston, W.J. Frederick, M.R. Nimlos, *Energy Fuels* 25 (2011) 324–336.
- [9] W. Jablonski, K.R. Gaston, M.R. Nimlos, D.L. Carpenter, C.J. Feik, S.D. Phillips, *Ind. Eng. Chem. Res.* 48 (2009) 10691–10701.
- [10] D.L. Carpenter, R.L. Bain, R.E. Davis, A. Dutta, C.J. Feik, K.R. Gaston, W. Jablonski, S.D. Phillips, M.R. Nimlos, *Ind. Eng. Chem. Res.* 49 (2010) 1859–1871.
- [11] R.J. Evans, T.A. Milne, *Energy Fuels* 1 (1987) 123–137.
- [12] A.M. Scheer, C. Mukarakate, D.J. Robichaud, G.B. Ellison, M.R. Nimlos, *J. Phys. Chem. A* 114 (2010) 9043–9056.
- [13] A. Vasiliou, M.R. Nimlos, J.W. Daily, G.B. Ellison, *J. Phys. Chem. A* (2009) 8540–8547.
- [14] K.R. Gaston, P. Pepiot, M.R. Nimlos, M.W. Jarvis, K.M. Smith, W.J. Frederick, *Energy Fuels* 25 (2011) 3747–3757.
- [15] C. Dupont, G. Boissonnet, J.-M. Seller, P. Gauthier, D. Schweich, *Fuel* 86 (2007) 32–40.
- [16] T.J. Haas, M.R. Nimlos, B.S. Donohoe, *Energy Fuels* 23 (2009) 3810–3817.
- [17] G. Blanquart, P. Pepiot-Desjardins, H. Pitsch, *Combust. Flame* 156 (2009) 588–607.
- [18] A. Busciglio, G. Vella, G. Micale, L. Rizzuti, *Chem. Eng. J.* (2008) 398–413.
- [19] A. Busciglio, G. Vella, G. Micale, L. Rizzuti, *Chem. Eng. J.* 148 (2009) 145–163.
- [20] P. Pepiot, O. Desjardins, *Powder Technol.* (2011), doi:10.1016/j.powtec.2011.09.021, online.
- [21] M.M. Yung, K.A. Magrini-Bair, Y.O. Parent, D.L. Carpenter, C.J. Feik, K.R. Gaston, M.D. Pomeroy, S.D. Phillips, *Catal. Lett.* 134 (2010) 242–249.
- [22] K.A. Magrini-Bair, S. Czernik, R. French, Y.O. Parent, E. Chornet, D.C. Dayton, C. Feik, R. Bain, *Appl. Catal. A-Gen.* 318 (2007) 199–206.
- [23] R.L. Bain, D.C. Dayton, D.L. Carpenter, S.R. Czernik, C.J. Feik, R.J. French, K.A. Magrini-Bair, S.D. Phillips, *Ind. Eng. Chem. Res.* 44 (2005) 7945–7956.
- [24] S. Czernik, R. French, C. Feik, E. Chornet, *Ind. Eng. Chem. Res.* 41 (2002) 4209–4215.
- [25] J. Hepola, J. McCarty, G. Krishnan, V. Wong, *Appl. Catal. B-Environ.* 20 (1999) 191–203.
- [26] M. Ashrafi, C. Pfeifer, T. Proell, H. Hofbauer, *Energy Fuels* 22 (2008) 4190–4195.
- [27] J. Hepola, P. Simell, *Appl. Catal. B-Environ.* 14 (1997) 305–321.
- [28] C. Lombard, S. Le Doze, E. Marenca, P.-M. Marquaire, D. LeNoc, G. Bertrand, Lapique, *Int. J. Hydrogen Energy* 31 (2006) 437.
- [29] J.R. Rostrup-Nielsen, *J. Catal.* 21 (1971) 171–178.
- [30] H. Oudghiri-Hassani, N. Abatzoglou, S. Rakass, P. Rowntree, *J. Power Sources* 171 (2007) 811–817.
- [31] C.H. Bartholomew, P.K. Agrawal, J.R. Katzer, *Adv. Catal.* 31 (1982) 135–242.
- [32] V. Subramani, S.K. Gangwal, *Energy Fuels* 22 (2008) 814–839.
- [33] J.J. Spivey, A. Egbebi, *Chem. Soc. Rev.* 36 (2007) 1514–1528.
- [34] S. Phillips, A. Aden, J. Jechura, D. Dayton, T. Eggeman, *Thermochemical Ethanol via Indirect Gasification and Mixed Alcohol Synthesis of Lignocellulosic Biomass*, National Renewable Energy Laboratory, Golden, 2007, p. 132.
- [35] A. Dutta, M. Talmadge, J.E. Hensley, M. Worley, D. Dudgeon, D. Barton, P. Groenendijk, D. Ferrari, B. Stears, *Process Design and Economics for Conversion of Lignocellulosic Biomass to Ethanol*, National Renewable Energy Laboratory, Golden, 2011, p. 175.